NASA TECHNICAL TRANSLATION NASA TT F-14,052

FUNDAMENTAL CONSIDERATIONS ON SPINEL FORMATION IN SCALE LAYERS AND ON THE TRANSPORT PROPERTIES OF THE SPINELS

H. Schmalzried

Translation of: "Grundsätzliche Über legungen zur Spinellbildung in Zunderschichten und zu den Transporteigenschaften der Spinelle", Werkstoffe und Korrosion, Vol. 22, No. 5, May 1971, pp. 371-382.

NATIONAL AERONAUTICS AND SPACE ADMINISTRATION
WASHINGTON, D. C. 20546 DECEMBER 1971

FUNDAMENTAL CONSIDERATIONS ON SPINEL FORMATION IN SCALE LAYERS AND ON THE TRANSPORT PROPERTIES OF THE SPINELS

H. Schmalzried[1]

ABSTRACT. Alloy oxidation is investigated for a certain phase configuration of the ternary system A-B-O. The structure, range of homogeneity, thermodynamics and defect concentrations of spinels are discussed for numerous examples. The formation of stable coating layers is described.

1. INTRODUCTION

/371*

The formation of coatings on pure metals through oxidation is really understood only for a few limiting cases. A series of rate laws have been found experimentally. The most important of these can be characterized as logarithmic, inversely logarithmic, linear, cubic, and parabolic [1]. The first-mentioned in particular are observed in very thin beginning layers. They have explanations, but the validity of these explanations is not unambiguously demonstrable because of the lack of independent determination of the constants appearing in the theories. Only the parabolic law of metal oxidation, which is well known from Tammann [2] and Pilling and Bedworth [3], and which describes the case which is by far the most important of the heterogeneous reactions of the type $Me(s) + \nu/2\ O_2(g) = MeO\nu(s)$, can be considered essentially understood in its theoretical explanation by Wagner [4]. With the hypothesis that local equilibrium is maintained during the entire process of scale formation both at the phase boundaries $Me/MeO\nu$ and $MeO\nu/O_2(g)$ and in the compact, solidly adhering scale layer, we obtain for the increase of layer thickness Δx the rate law

*Numbers in the margin indicate pagination in the original foreign text.

[1]Institute for Theoretical Metallurgy of the Technical University, Clausthal.

$$\Delta x^2 = 2\bar{k}t \quad (1)$$

where $\bar{k}$ is the practical (Tammann) scale constant. In the oxidation of most metals, coatings are formed having transport numbers of nearly one for electronic charge carriers. Furthermore, the diffusion coefficients of the cations in the coatings are often significantly larger than those of the anions, especially if we are dealing with an oxygen ion sub-lattice of nearly the densest packing. Then the calculation yields a very simple expression for the practical reaction constant $\bar{k}$ [5]

$$\bar{k} = \bar{D}_{Me} \cdot \Delta G_{MeO}/RT \quad (2)$$

Thus $\bar{k}$ contains the component diffusion coefficient $\bar{D}$ averaged over the reaction layer and the driving force ΔG_{MeO} divided by the thermal energy RT for the scaling reaction $Me + 1/2\ O_2 = MeO$.

If we go from the oxidation of pure metals to the oxidation of alloys, and again hypothesize that local equilibrium is maintained, then considerations of limiting cases must help to organize the profusion of potential reaction types [22]. The following parameters will define the oxidation behavior of an alloy being considered: the activities of the components in the alloy and oxide phases, and especially the values of the free enthalpies of formation of the individual oxides from the elements. The transport coefficients in the alloy and coating are also important for the mechanism of alloy oxidation. It is pre-supposed again that compact and adherent layers form. With the ratios of molar volumes of metal and oxide, this requires the maintenance of plastic flow within certain limits. Here we shall merely comment that more detailed deliberations must be modified by additional complications, such as the phenomenon of internal oxidation or the occurrence of pores due to vacancy site oversaturation and lack of plastic flow.

If we limit ourselves at first to binary alloys, even though they do not occur frequently in technology, then from the great number of potential types

of ternary phase diagrams A-B-O we quickly recognize the necessity of introducing model systems in order to maintain the ability to survey the field. /372
Model systems were introduced even in the most important fundamental investigations of alloy oxidations which have yet appeared [6].

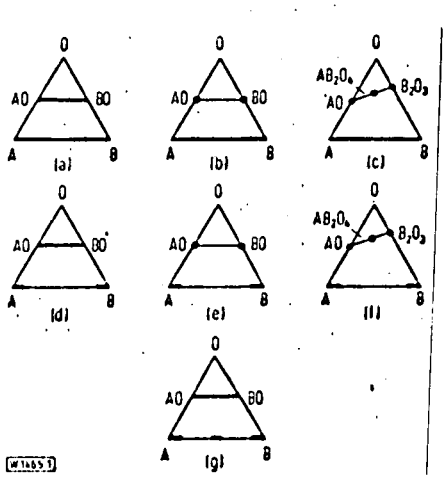

Figure 1. The phase distributions of metals and oxides in the ternary system A-B-O which are most important for alloy oxidation.

The phase distributions which are most important for alloy oxidation are plotted in Figure 1, where the presentation is in the Gibbs phase triangle A-B-O. Later figures will explain how alloy oxidation is discussed by means of tie lines in these or similar phase diagrams. Here it is enough to say that the tie lines and thus the equilibrium regions depend very basically on the values of ΔG°_{AO} and ΔG°_{BO} or ΔG°_{B2O3}. Wagner [7] has recently undertaken fundamental deliberations on alloy oxidation for the case of Figure 1,a. The case of Figure 1,b has already been worked on in earlier works of Wagner [8, 9]. It is common to both cases that the metal phase always remains a single phase during the oxidation. This is different in cases 1,d to 1,g. Here, an alloy which is at first assumed to be a single phase can become several phases during the course of oxidation. As an example, a work by Wagner [28] may be mentioned. Similar very fundamental investigations as for cases 1,a and 1,b have not yet been undertaken.

In this work, we shall study essentially the alloy oxidation of the case of Figure 1,c. Here it will be assumed that a spinel phase AB_2O_4 appears, although further deliberations also apply to phase diagrams with other ternary compounds.

2. CHARACTERIZATION OF SPINELS

2.1 Structure

Spinels are double oxides with the composition $AO \cdot B_2O_3$ or $2\ AO \cdot BO_2$. $MgAl_2O_4$ is the prototype which gave this class of compounds its name. Spinels belong to the structurally simplest ternary ionic crystals. The anion sublattice consists of a face-centered cubic, nearly tightest packing of oxygen ions. The various cations are accommodated in the tetrahedrally and octahedrally coordinated interstices of the anion lattice. Two limiting cases of cation distribution have received special names: we speak of a normal spinel if the bivalent cations occupy one eighth of the total tetrahedral sites present in a quite definite way, and if twice as many of the trivalent cations occupy half of the total octahedral sites present. We speak of an inverse spinel if, instead of the bivalent cations, half of the trivalent cations are statistically distributed in the octahedral sites. These relations are shown for survey in Figure 2 [10].

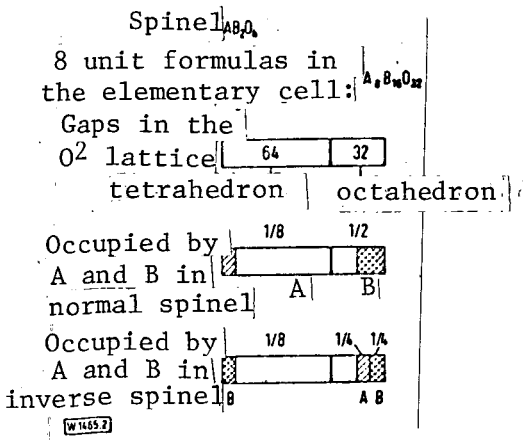

Figure 2. The distribution of cations among octahedral and tetrahedral sites in spinel phases.

A large number of spinel phases consist of transition metal oxides, or contain them. Thus they show predominantly excess or defect electron conductivity. Then there arises not only the problem of the cation distribution among the crystallographic sites present, as described above for the two limiting cases, but also the problem of the distribution of the charges of the same cations, which are accommodated in the same or different sublattices. The simplest example is the charge distribution in magnetite, Fe_3O_4, which

crystallizes in the spinel structure. Since only iron ions appear as cations, only their charge distribution is open to question. An inverse spinel would occur if the limiting distribution of the charges were Fe_A^{3+} $[Fe_B^{2+}\ Fe_B^{3+}]\ O_4$. Here the index A designates tetrahedral sites, and index B designates octahedral sites. In comparison, magnetite as a normal spinel would be characterized by the formula $Fe_A^{2+}\ [Fe_B^{3+}\ Fe_B^{3+}]\ O_4$. The distribution of the cations and charges among the sites prescribed by the structure also determines to a great degree the transport properties of the spinels, as is yet to be shown below. Reference [11] summarizes a literature review on cation and charge distributions in spinels.

2.2 Range of Homogeneity

Ion and electron transport in solid compounds depends on their lattice defects. Aside from thermal lattice defects of compounds with stoichiometric compositions, we shall mention in particular the lattice defects which occur from excess solution of the components of these compounds, or from solution of foreign components in these compounds. Solubility of their own or foreign oxides is also possible for spinel phases within their ranges of homogeneity. Spinels are mutually soluble to the greatest extent at appropriate temperatures and oxygen partial pressures [12]. As examples, we may mention the completely miscible phases between $CoFe_2O_4$ and Fe_3O_4 or those between $NiAl_2O_4$ and $CoCr_2O_4$ at temperatures above 1000° C.

The individual oxides AO and B_2O_3 are also in many cases quite considerably soluble in the double compound AB_2O_4. As examples, we mention (1) the quasibinary system $FeO\text{-}Cr_2O_3$ with approximately 20% excess solubility of FeO in $FeCr_2O_4$ at 1300° C [13] or (2) the quasibinary system $MgO\text{-}Al_2O_3$ with a similarly great excess solubility of Al_2O_3 in $MgAl_2O_4$ at 1400° C [14]. Other spinels such as $NiCrO_4$ have a very narrow range of homogeneity up to 1300° C [35]. /373

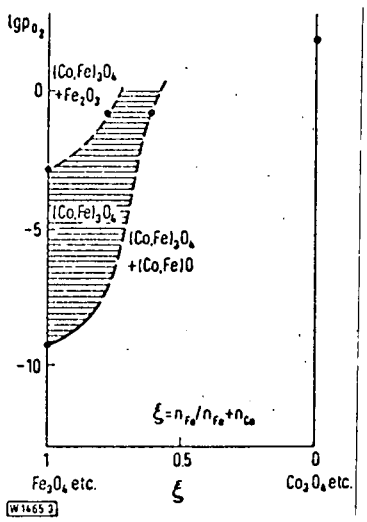

Figure 3. The range of homogeneity of cobalt ferrite as a function of the partial pressure of oxygen at 1180° C.

Establishing the fact that the expansion of homogeneity ranges in spinels with transition metal cations depends on the oxygen partial pressure is certainly important in relation to the occurrence of spinels in scale layers. The case of cobalt ferrite is plotted in Figure 3 as an example [19].

The phase boundary lines can be calculated if the cation distribution among the lattice sites is known and if it is assumed that the free enthalpy of the spinel phase is a linear combination of the concentration contributions from all the cation phases occurring. Therefore we may conclude for such a spinel in the scale layer that its composition can vary, depending on the place at which it occurs in the scale.

Just as simple binary transition metal oxides show a cation excess or deficiency depending on the oxygen partial pressure (example: $Fe_{1}\Delta O$ or $Fe_{3}\Delta O_{4}$), there also are ternary oxide spinels with deviations from the ideal metal/nonmetal ratio, if they contain transition metal cations. That is, they have an excess or a deficiency of cations. By way of explanation, there is plotted in Figure 4 the cation deficiency Δ as a function of the cobalt content x, i.e., the range of existence of the mixed phase in relation to oxygen, for the ternary mixed phase $Co_xFe_{3-x}\Delta O_4$ [15]. From Figure 4 we can see that, starting from magnetite, $Fe_3\Delta O_4$, the cation deficiency decreases with increasing cobalt content in the spinel phase. Since Δ describes the cation vacancy site concentration, which enters the diffusion coefficient as a determining quantity, the knowledge of Δ is essential for calculating the average transport coefficients in scale layers.

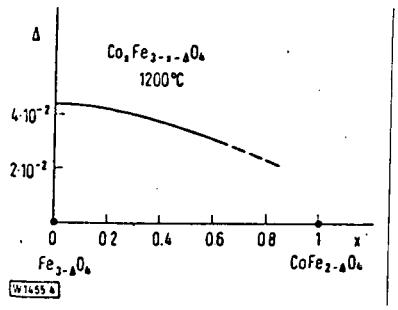

Figure 4. The cation deficiency Δ as a function of the composition of cobalt ferrite in equilibrium with hematite.

2.3 Thermodynamics

Let it be assumed that in the quasibinary system Ao-B_2O_2 there is only the one compound AB_2O_4 with spinel structure. Then through solid body reaction between Ao and B_2O_3 we obtain the spinel phase by the reaction equation

$$AO + B_2O_3 = AB_2O_4, \quad \Delta G^\circ_{AB_2O_4} \tag{3}$$

as long as the oxygen partial pressure is selected so that all three oxides can mutually coexist. By means of solid body galvanic cells and other measuring methods, a large number of values of $\Delta G^\circ_{AB_2O_4}$ have now been determined for spinel phases. A selection is summarized in Table 1 [16].

TABLE 1. FREE ENTHALPIES OF FORMATION, $\Delta G^\circ_{AB_2O_4}$ at 1000° C

A	ACr_2O_4	AAl_2O_4	AFe_2O_4
Fe	- 8,75 ± 0,2	- 5.7 ± 0,2	- 7,5 ± 0,25
Co	- 6,4 ± 0,5	- 7.3 ± 0,4	- 9.4
Ni	- 9,9 ± 0,4	- 4,4 ± 0,4	- 6,0 ± 0,3
Cu	- 12,0 ± 0,2		
Mg	- 8,1 ± 0,5	- 8,4	- 5,3 ± 0,4

As can be seen, at 1000° C the $\Delta G^\circ_{AB_2O_4}$ values on the whole vary between -5 and -10 kcal per mole for the various formulas. Then, after explicit application of the equilibrium condition to Equation (3), this yields

$$a_{AO} \cdot a_{B_2O_3} = \exp \Delta G^\circ_{AB_2O_4} / RT \tag{4}$$

From this it follows that the activity of the initial oxide Ao and B_2O_3 varies between 1 and 0.1 within the homogeneity range of the spinel phase, while the product of these activities must always obey Equation (4). If the activity of AO or B_2O_3 is significantly smaller than 0.1, no spinel phase will be able to form.

2.4 Lattice Defect Concentrations as a Function of Independent Thermodynamic Variables

In a crystalline compound of n elements, the equilibrium concentrations of point defects depend not only on P and T, but also on (n - 1) component activities. It is already known in binary oxides that the concentrations of point defects (e. g., of the cation vacancy sites in $Ni_{1-\Delta}O$) are proportional to $a_0^{1/n}$. Here a_0 indicates the oxygen activity and n is a numerical factor related to the type of lattice defect and the stoichiometry. It is easily derivable by means of lattice defect thermodynamics [17]. In a binary oxide, then, all the lattice defect concent ations are established unambiguously by P, T, and a_0. In the ternary spinel AB_2O_4, in contrast, there is still one more independent variable. As long as we have not been able to establish with sufficient accuracy the composition in compounds with narrow homogeneity ranges, it has proved expedient to introduce the oxygen partial pressure and therefore the activity of a single oxide, such as a_{AO}, as the independent component activity for ternary oxides. If we designate the component activities generally as a_i, then it can be shown even for higher ionic crystals [18] that the concentrations of point defects (F) depend on the component activities in the following way:

/374

$$(F) = K \cdot (a_i^{1/n}), \quad P, T, a_{j \neq i} = \text{const} \tag{5}$$

On the other hand, it appears, on the basis of the usual assumption of ideal behavior of the point defects in their sublattices, that n depends on the type of lattice defect and on the stoichiometry of the ternary compounds under consideration. To be sure, the number of possible types of lattice defects (as a combination of both majority lattice defect centers) is far higher than in the case of binary compounds, as a glance at Table 2 shows. Even though unambiguous determination of the lattice disorder type in binary ionic compounds is a difficult undertaking, this is even more true for ternary compounds, so that only a few lattice disorder types have been definitely established in spinels to date [18].

TABLE 2. LATTICE DEFECT TYPES IN TERNARY IONIC CRYSTALS AB_2O_4 WITH PURELY IONIC LATTICE DEFECTS.

	A_Z''	B_Z'''	V_A''	V_B'''	A_B'	B_A'	V_O''	O_Z''
A_Z''			±	+A	+A			+A
B_Z'''			+B	±	+B			+B
V_A''						+B	+B	
V_B'''						+B	+A	
A_B'						±	+A	
B_A'								+B
V_O''								±
O_Z''								

Explanation: The lattice disorder centers listed in the rows and columns are the majority lattice disorder centers for the lattice disorder type. ± indicates thermal lattice disorder with a slight excess solubility of either AO or B_2O_3.
+A indicates excess solubility of AO
+B indicates excess solubility of B_2O_3.

The transport of lattice elements is only possible via lattice defects. In a volume diffusion region, until the present the assumption has been extensively maintained that the transport coefficients and so also the component diffusion coefficients are proportional to the concentration of those lattice defect types which mediate transport in the lattice. Thus we obtain, along with Equation (5), this equation for the component diffusion coefficient of A in spinels:

$$D_A = D^\circ_A \cdot (a_j/a_j^\circ)^{1/n}, \quad P, T, a_{j\neq i} = \text{const} \qquad (6)$$

Here the notation ° indicates an arbitrarily selected reference state. Analogous equations apply for the other component diffusion coefficients. Table 3 shows the ratios of component diffusion coefficients $D_A(B_2O_3)/D_A(AO)$ at constant pO_2, calculated from Equation (6) on the basis of lattice defect thermodynamics for all the possible cation lattice disorder types in spinels (see Table 2). The components B_2O_3 or AO in parentheses indicate that the spinel is to be considered in equilibrium with B_2O_3 or AO. Here it is assumed that $\Delta G^\circ_{AB_2O_4}$ is -6 kcal. According to Equation (4), this indicates that the value 0.14 states the ratio of AO activities $a_{AO}(B_2O_3)/a_{AO}(AO)$ at the limit of the homogeneity range at 1250° C.

Just as the dependence of lattice defect concentrations or diffusion coefficients on a_{AO} can be calculated and tabulated at constant pO_2, so can

TABLE 3. THE RATIO $D_A(B_2O_3)/D_A(AO)$ AND $D_B(B_2O_3)/D_B(AO)$ FOR SPINELS AT THE LIMITS OF THEIR HOMOGENEITY RANGES AT T = 1250° C AND $\Delta G°_{AB_2O_4}$ = -6 kcal.

Lattice disorder type	Interlattice diffusion	Vacancy site diffusion	Interlattice diffusion	Vacancy site diffusion
$A_Z^{\cdot\cdot}$, $V_B^{'''}$	0,21	4,8	4,8	0,21
$A_Z^{\cdot\cdot}$, $A_B^{'}$	0,071	14	1	1
$B_Z^{\cdot\cdot\cdot}$, $A_B^{'}$	0,019	53	0,14	7,2
$A_Z^{\cdot\cdot}$ $A_A^{''}$	1,00	1	53	0,019
$A_B^{'}$, $B_A^{\cdot}$	0,00036	2780	0,00036	2780
$B_Z^{\cdot\cdot\cdot}$, $V_B^{'''}$	0,071	14	1	1
$B_Z^{\cdot\cdot\cdot}$, $V_A^{''}$	0,21	4,8	4,8	0,21
$B_A^{\cdot}$, $V_B^{'''}$	0,019	53	0,14	7,2
$B_A^{\cdot}$, $V_A^{''}$	0,071	14	1	1

their dependence on pO_2 at constant a_{AO} be calculated and tabulated. In systems with pure cationic lattice disorder, as in $MgAl_2O_4$ or $NiAl_2O_4$ we expect no dependence of the concentration of the majority lattice disorder centers on the oxygen partial pressure. This simplifies many deliberations on the transport properties of spinels in scale layers. In systems with an electronic majority lattice disorder center, there is a dependence like that of Equation (5) or (6). To be sure, it can quite generally be established that the exponents 1/n are smaller than in the case with variable a_{AO} discussed above. In spite of this, the variation of lattice defect concentrations can be just as large or even larger than shown in Table 3, because the range of variation for p_{O_2} is usually much greater than is that of a_{AO} (see also Figure 5).

2.5 Examples for Diffusion in Spinels

For cobalt ferrite $Co_{1-x}Fe_{2+x}O_4$, cation diffusion coefficients have been /375

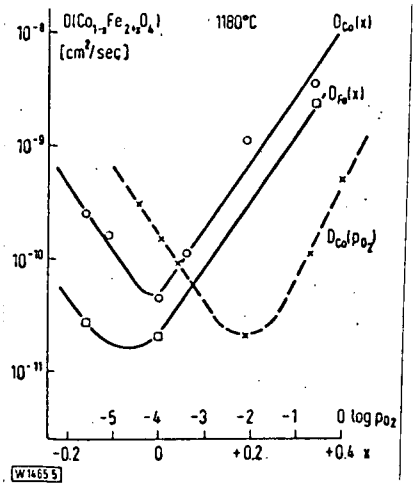

Figure 5. The tracer diffusion coefficients of cobalt and iron in cobalt ferrite as a function of the composition and of the oxygen partial pressure.

measured as a function of the activity of CoO and as a function of the oxygen partial pressure. These measurements can explain the generally maintained deliberations of the previous section. First it must be established that cobalt ferrite is stable in air at 1180° C within the approximate limits $Co_{0.66}Fe_{2.34}O_4$ - $Co_{1.16}Fe_{1.48}O_4$. For other oxygen partial pressures, the limits of the homogeneity range shift (see also Figure 3). Electrical conductivity measurements indicate that $CoFe_2O_4$ is basically an inverse spinel. But then, according to Table 3, we must expect a strong dependence of the transport coefficients on the activity of cobalt oxide. Figure 5 shows the self-diffusion coefficient of both cobalt and iron as functions of the composition x ($Co_{1-x}Fe_{2+x}O_4$) and the self-diffusion coefficient of cobalt as a function of pO_2 for x = 0.063. It is at first striking that D_{Co} passes through a minimum at about the stoichiometric composition for the spinel, $CoFe_2O_4$, and climbs sharply for excess of iron as well as of cobalt (by a factor of about 100 for x > 0). We can conclude from this that there is predominantly vacancy site diffusion in the range x < 0 and interlattice diffusion in the range x > 0. The dependence of cobalt diffusion on the oxygen partial pressure also shows a change in the diffusion mechanism. The theoretical considerations are quite well confirmed, as well as the dependence of the self-diffusion coefficients on a_{CoO} as well as on pO_2.

/376

As a further example, the tracer diffusion coefficient of manganese in manganese ferrite $Mn_xFe_{3-x}O_4$ at 1440° C in air is plotted in Figure 6 as a function of the composition [23]. In contrast to cobalt ferrite, here the diffusion coefficient changes only a little. If we assume that above 1300° C,

where Fe_3O_4 and Mn_3O_4 are completely miscible in air, there is a statistical distribution of cation types among the available regular cation sites, then it should be true that

$$D_{Mn}(x) \approx D_{Mn} \quad (x = 0)$$

as long as the transition frequencies of the ions are independent of the composition. As Figure 6 shows, this is approximately the case.

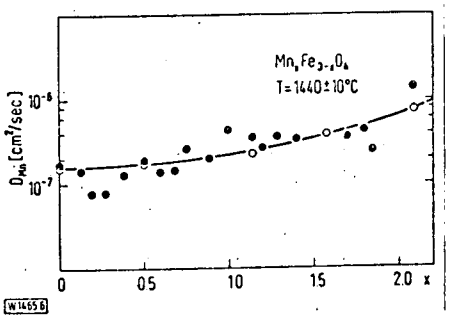

Figure 6. The tracer diffusion coefficient of manganese in manganese ferrite in air as a function of the composition.

In Figure 7, furthermore, most of the tracer diffusion coefficients which have so far become known for spinels as a function of the temperature are shown. For comparison, Figure 8 shows tracer diffusion coefficients of binary oxides. The few measured values given by several authors for the same substance show that the discrepancies are often considerable. The reason may be in the fact that generally no unambiguous determination of component activities was undertaken. In this relation, we may refer expressly to curves 19, 20, and 21 in Figure 7, which show the strong dependence of the tracer diffusion coefficients on the component activities. On the other hand, the fact that spinels usually occur as porous polycrystalline materials certainly has an effect, so that it is difficult to say whether the volume diffusion coefficients were actually determined. In Figure 7, the diffusion coefficients are plotted for the temperature range of particular interest for oxidation processes. For this purpose they are in part extrapolated from higher experimental temperatures. In all, it can be established that the ionic mobilities measured so far are lowest for aluminate and higher for chromite. The highest diffusion coefficients are found in the ferrites. This is certainly based on the high cation deficit and the related high vacancy site concentration.

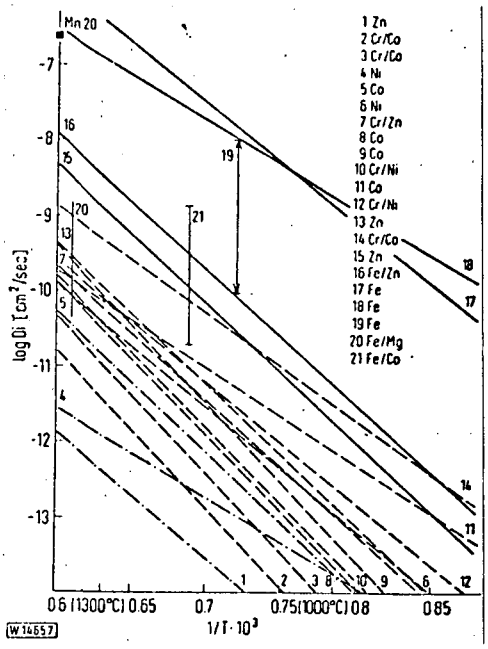

Figure 7. Tracer diffusion coefficients of various spinels corresponding to the attached collection of citations.

- · - · - Aluminate

--------- Chromite

———— Ferrite

Explanations for Figure 7

Cation tracer diffusion coefficient of different spinels:

1)	$ZnAl_2O_4$	*R. Lindner, A. Akerström:* Z. phys. Chem. NF 6, 162 (1956)
2)	$CoCr_2O_4$ (+CoO)	*A. Morkel, H. Schmalzried:* Z. phys. Chem. NF 32, 76 (1962)
3)	$CoCr_2O_4$ ($+Cr_2O_3$)	*A. Morkel, H. Schmalzried:* Z. phys. Chem. NF 32, 76 (1962)
4)	$NiAl_2O_4$	*R. Lindner:* Proc. 2. Int. Conf. Peaceful Uses Atomic Energy 20, 116 (1958)
5)	$CoAl_2O_4$	See 2)
6)	$NiCr_2O_4$	See 1)
7)	$ZnCr_2O_4$	"
8)	$CoCr_2O_4$ ($+Cr_2O_3$)	See 2)
9)	$CoCr_2O_4$ (+CoO)	"
10)	$NiCr_2O_4$	"
11)	$CoCr_2O_4$	*R. Sun:* J. Chem. Phys. 28, 290 (1958)
12)	$NiCr_2O_4$	See 1)
13)	$ZnCr_2O_4$	"
14)	$CoCr_2O_4$	See 11)
15)	$ZnFe_2O_4$	*R. Lindner et al.:* Acta Chem. Scand. 6, 457 (1952)
16)	$ZnFe_2O_4$	*R. Lindner:* Z. Naturforschg. 10 a, 1027 (1955)
17)	Fe_3O_4	*S. M. Klotsman et al.:* Fiz. Metal. y. Met. 10, 733 (1960)
18)	Fe_3O_4	*L. Himmel, R. F. Mehl, C. E. Birchenall:* Trans. AIME 197, 827 (1953)
19)	Fe_3O_4	*H. Schmalzried:* Z. phys. Chem. NF 31, 184 (1962)
20)	$MnFe_2O_4$	*H. H. Hohmann et al.:* Proc. Brit. Cer. Soc. 8, 91 (1967)
21)	$CoFe_2O_4$	*W. Müller, H. Schmalzried:* Ber. Bunsenges. phys. Chemie 68, 270 (1964)

Explanation: The first element symbol at a line indicates the measured tracer diffusion coefficient, e.g., --- Co = cobalt measured in cobalt chromite. In comparison, --- Cr/Ni indicates that the value of the chromium diffusion coefficient of nickel chromite was plotted.

Deductions which attempt to determine unknown diffusion coefficients in spinels by comparison of already measured diffusion coefficients are to be evaluated with great reservations. Too many parameters are operating. The most important of these are: vacancy site concentration (dependent on the component activities), cation distribution (normal, inverse, statistic) and fusion temperature. In this relation, to evaluate the effectiveness of corrosion protection from spinels to note the fact that part of the ferrite shows higher cation mobility than NiO or Cr_2O_3, to say nothing of Al_2O_3. It is not to be expected that ferrites, which occur

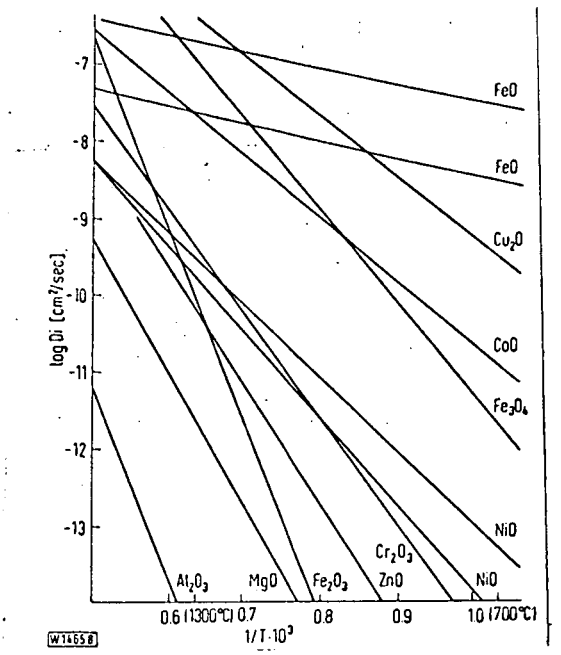

Figure 8. Tracer diffusion coefficients of various binary oxides, corresponding to the attached collection of citations.

Citations to Figure 8

Cation tracer diffusion coefficients of binary oxides:

Al_2O_3 *A. E. Paladino, W. D. Kingery:* J. chem. Phys. *37*, 957 (1962)
MgO *R. Lindner, C. D. Parfitt:* J. chem. Phys. *26*, 182 (1957)
Fe_2O_3 *R. Lindner:* Arkiv Kemi *4*, 381 (1952)
ZnO *R. Lindner et al.:* Acta Chem. Scand. *6*, 457 (1952)
Cr_2O_3 *W. G. Hagel, A. U. Seybolt:* J. Electrochem. Soc. *108*, 1146 (1961)
NiO *R. Lindner, A. Akerström:* Disc. Faraday Soc. *23*, 133 (1957)
NiO *M. T. Shim, W. J. Moore:* J. chem. Phys. *26*, 802 (1957)
Fe_3O_4 *L. Himmel, R. F. Mehl, C. E. Birchenall:* Trans. AIME *197*, 827 (1953)
CoO *W. K. Chen et al.:* Phys. Rev. *186*, 887 (1969)
Cu_2O *W. J. Moore et al.:* J. Phys. Chem. *62*, 1438 (1958)
FeO *E. F. Carter, F. D. Richardson:* Trans. AIME *200*, 1244 (1954)
FeO *L. Himmel, R. F. Mehl, C. E. Birchenall:* Trans. AIME *197*, 827 (1953)

in scale layers along with the last-named oxides, will show a protective action.

2.6 The Influence of Doping on Spinel Lattice Disorder

At the very beginning of this section it must be established that there are no systematic studies of the influence of doping with foreign materials on lattice disorder in ternary ionic crystals. But a series of general statements can be made on the basis of experience with binary ionic crystals, and by means of lattice disorder theory for ternary ionic crystals, concerning just this effect.

If one has a solid solution AO-BO, such as CoO-MgO or NiO-MgO, it is known that the concentration of cation vacancies at constant oxygen partial pressure decreases about exponentially with the increase of MgO [29]. The result of this is that the diffusion coefficients of the cations in such systems decrease correspondingly [30]. It will be shown shortly that solid solutions of ternary oxides behave quite analogously (e.g., $CoAl_2O_4$ - $MgAl_2O_4$).

Of the dosing of binary ionic crystals, it is known that by means of heterovalent additives, one can vary the concentration of point defects which occur in thermodynamic equilibrium. Thus, for example, one speaks of controlled valence if the number of excess or deficient electrons is adjusted by cations of different valence. (Example: $Ni_{NI}3+$ in NiO by means of $Li_{Ni}+$.) In ionically conducting crystals, one can in just the same way adjust the number of vacancy sites or interstitial ions by dosing (example: V''_{Mg} in MgO by $Cr_{Mg}+3$). It is common for this process that with sufficient solubility, the particles of the dosing agent become majority lattice disorder centers within their solubility range, while the second type of complementary lattice disorder centers are maintained by inherent lattice disorder. The center always has the smallest lattice disorder energy.

Conditions are completely analogous for ternary ionic crystals. The difficulty in comparison to binary crystals is to be found only in the far larger number of possible types of lattice disorder. The result is that until the present no general prediction on the action of a particular dosant on a certain ternary compound has been possible. General guidelines can be given, however. Let us assume that we have a spinel with one type of cation lattice disorder. Then we find ourselves in the quasibinary system $AO-B_2O_3$, and the deviation from stoichiometric composition can be expressed as $A_{1-x}B_{2+2/3x}O_4$. Expressed differently, according to the appropriate phase diagram, a certain amount of AO or B_2O_3 is dissolved in AB_2O_4. The lattice disorder types possible in this way have already been summarized in Table 2. Now if we dose with A'O or B'_2O_3, i.e., with oxides of bivalent or trivalent foreign cations, then in general, within the given solubility limits, A'O will have the same effect as an excess of AO and B'_2O_3, or as an excess of B_2O_2 in the spinel. This situation is portrayed graphically in Figure 9. For example, if we have, in the normal spinel $MgCr_2O_4$ with a cation deficit, the lattice disorder type $(Cr_Z) \simeq 2/3\ (V''_{Mg})$, then it can be assumed that an addition of Al_2O_3 to $MgCr_2O_4$ will produce the same type of lattice disorder. Of course, there is the presumption that the trivalent dosing ion goes to the octahedral positions of the normal spinel and that the bivalent dosing ions

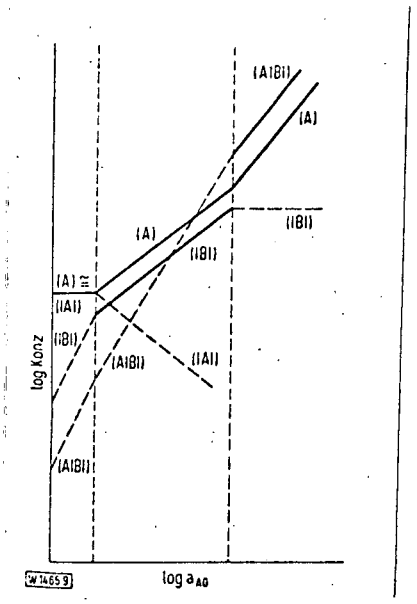

Figure 9. The activity dependence of lattice disorder concentrations in spinels. A indicates interstitial particles, and |A| vacancy sites. (A) ≃ (|A|) is the condition for Frenkel defects in the A sublattice.

go to the tetrahedral positions of the normal spinel. Otherwise, the lattice disorder types resulting from dosing can not be so simply predicted. The same is true, naturally, for the inverse spinels. Thus, for example, one would expect that addition of MgO to $CoFe_2O_4$, for which the lattice disorder has already been discussed in Section 2.5, would act just the same as if one were to dissolve CoO in excess. Based on Figure 5, then, an increase of the self-diffusion coefficients of Co and Fe would be the result in each case.

If one wishes to know in detail the dependence of the point defect concentrations on dosing, then he must explicitly compute the point defect concentration as a function of the dosant concentration according to the procedure given in [18], considering space balance, charge balance, and internal lattice defect equilibrium. This applies not only for spinels with a purely cationic lattice disorder type, but also for spinels in which there are electronic majority lattice disorder centers.

3. COATING FORMATION AS AFFECTED BY SPINELS

3.1 Equilibrium Regions in the Phase Diagram

Let us begin with the phase diagram of Figure 1,c, on which the following discussions will be based. First we shall inquire about the tie lines and the equilibrium regions. Let the values ΔG°_{AO}, ΔG°_{B2O3} and ΔG°_{AB2O4} be given. Let it also be assumed that the alloy behaves ideally. Deviations from

ideality can be considered simply by introduction of the proper activity coefficients. They do not otherwise change the basic considerations. Two limiting cases are to be differentiated: (1) $|3 \cdot \Delta G^\circ_{AO}| >$ or $>> |\Delta G^\circ_{B2O3}|$ and (2) $|3 \cdot \Delta G^\circ_{AO}| <$ or $<< |\Delta G^\circ_{B2O3}|$. If case 1 is realized, then because of the high stability of AO, the oxide AO will be oxidized out of the alloy down to relatively low oxygen partial pressures. This results in a phase diagram of the type of Figure 10,a: AO and AB_2O_4 are in equilibrium with a B-rich alloy. Conversely, B_2O_3 and AB_2O_4 are in equilibrium with an A-rich alloy if case 2 is realized (see also Figure 10,b).

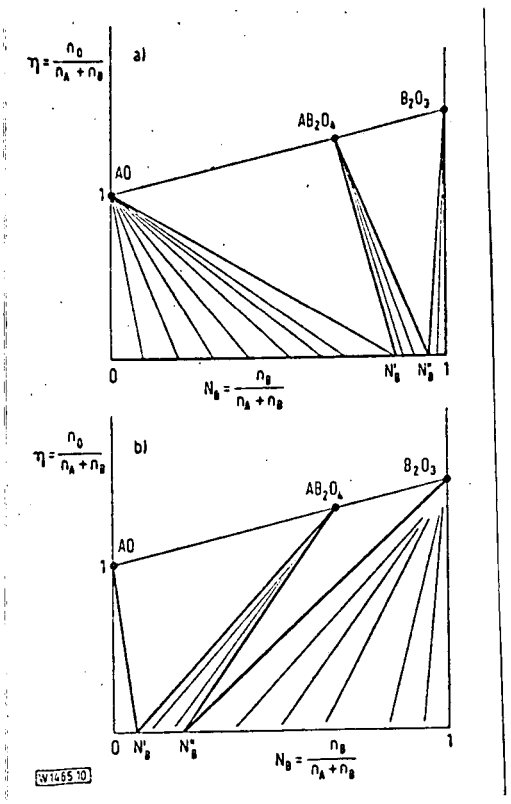

Figure 10. The phase diagram A-B-O for the case in which A-B are completely miscible and the oxides AO, B_2O_3 and AB_2O_4 occur.

a) $|3\Delta G^\circ_{AO}| > |\Delta G^\circ_{B_2O_3}|$ b) $|3\Delta G^\circ_{AO}| < |\Delta G^\circ_{B_2O_3}|$

In order to calculate the composition of the alloy for coexistence with AO and AB_2O_4 (N'_B) or with B_2O_3 and AB_2O_4 (N''_B), we consider the displacement reactions

$$2\,B + 4\,AO = AB_2O_4 + 3\,A \qquad (7)$$

or

$$3\,A + 4\,B_2O_3 = 3\,AB_2O_4 + 2\,B \qquad (8)$$

In the case of the coexistences stated, the equilibrium conditions apply for Equations (7) and (8). Considering the equilibrium conditions for the formation reactions of the individual oxides AO and B_2O_3 and the spinel formation reaction, Equation (3), we obtain directly the mole fractions N'_B or N''_B for the case of ideal behavior of the alloy:

$$N'_B{}^2 \cdot (1-N'_B)^{-3} = \exp - \frac{1}{RT}\left[+ 3\,\Delta G^\circ_{AO} - \Delta G^\circ_{B_2O_3} - \Delta G^\circ_{AB_2O_4}\right] \quad (9)$$

or

$$N''_B{}^2\,(1-N''_B)^{-3} = \exp - \frac{1}{RT}\left[3\,\Delta G^\circ_{AO} - \Delta G^\circ_{B_2O_3} + 3\,\Delta G^\circ AB_2O_4\right] \quad (10)$$

For understanding the later kinetic considerations, it is useful to establish that the spinel phase can coexist with the alloy between the mole fractions N'_B and N''_B. For example, if $|3\,\Delta G^\circ_{AO}| << |\Delta G^\circ B_2O_3|$, then N'_B and N''_B are << 1 so that

$$N''_B/N'_B = \exp - \frac{2\,\Delta G_{AB_2O_4}}{RT} \quad (11)$$

Therefore $N''_B > N'_B$, and the more so, the greater $\Delta G^\circ_{AB_2O_4}$ is. Furthermore, the remaining tie lines plotted in Figure 10 can easily be calculated by means of Equations (7) and (8) and the formation reactions for the individual oxides (see later). With introduction of the appropriate activity coefficients, the calculation can be performed similarly for non-ideal alloys.

3.2 General Considerations on Formation of a Surface Film

In order for flat, stable surface films to form in alloy oxidation, material transport in the alloy due to diffusion must be very fast in comparison to diffusion of ions in the oxide layer [20]. If the alloy composition, measured in N_A or N_B, does not have the extreme values 0 or 1, and if the molecular volumes of the alloy and oside do not differ too greatly, this means essentially that the necessary presumption for formation of a flat stable surface film, $D_{ME} > D_i$ (oxide) must apply. If, for example, we consider alloys of chromium with Fe, Co, and Ni, then this prerequisite must apply to some extent, as a comparison of cation diffusion coefficients in Cr_2O_3 and chromites (see Figure 7) with the chemical diffusion coefficients in the corresponding alloys shows [24]. We can proceed beyond this, because,

on the one hand, processes in the formation of unstable ternary surface films are theoretically extremely obscure, while, on the other hand, only continuously covering spinel layers, if any, promise effective protection against corrosion.

With the assumption of exclusively cationic diffusion in the semiconducting surface film, we can formulate the diffusion equations for the interiors of the individual phases in the usual manner and without difficulties [5]. Today, we know from studies on spinel formation as a solid state reaction that in general opposing cation diffusion appears as the reaction mechanism. From this we can conclude that the cation diffusion coefficients even in the spinel are large in comparison to the oxygen diffusion coefficients. In the alloy (A, B) the transport of metal atoms is regulated by a single chemical diffusion coefficient D_{Me}. In order to integrate the transport equations in the absence of knowledge about the rates of the phase boundary reactions, and to be able to apply them to the kinetic problems, we must assume that thermodynamic equilibrium is adjusted locally. In this way the component activities at the phase boundaries in the ternary systems are only partially established, however. The remaining conditions for fixing the component activities at the phase boundaries for calculating the kinetics can be obtained by means of the continuity equations. A quantitative calculation can hardly be mastered in its general form. For this reason we shall next discuss, by means of Figure 10, the case of alloy oxidation in which the metal phase (A, B) represents a semi-infinite space and $D_{Me} >> D_i$(oxide). Let the oxygen solubility in the metal be negligible.

The conditions given have the result that an activity a_A or a_B of the magnitude N°_A or N°_B appears and remains beyond the time $t = 0$ at the metal/oxide phase boundary. The courses of the tie lines can be calculated most simply as in Section 3.1. Then from the diagram one can read immediately what surface coating will form on an alloy of given composition. Since, according to the identity of the phase diagram, an alloy of definite

composition, neglecting singular points, can be in equilibrium with only one oxide, in this case the scale layer is a single phase.

Figure 11 shows a simple and practical representation of the situation for the case of Figure 10,a. The curve for log pO_2 (AO/[A, B] is calculated according to the equation /379

$$\log p_{O_2}(AO/[A, B]) = -2 \log (1-N_B) + \frac{2 \Delta G^\circ_{AO}}{RT} \quad (12)$$

from the equilibrium condition for $A + 1/2\ O_2 = AO$. Analogously, the curve for log pO_2 (B_2O_3/[A, B]) can be calculated. For the curve of log pO_2 (AB_2O_4/[A, B] we must combine Equation (7) with the equilibrium condition for $A + 1/2O_2 = AO$. This yields

$$\frac{1}{2RT}\left(\Delta G^\circ_{AO} + \Delta G^\circ_{B_2O_3} + \Delta G^\circ_{AB_2O_4}\right) \quad (13)$$

We note that log pO_2/N_B diagrams correspond throughout to the familiar T/N_B phase diagrams. As previously emphasized, it is assumed here and in further discussion that no internal oxidation processes complicate the curve [6]. Then, with the conditions established, a parabolic rate law is to be expected for the kinetics of the alloy oxidation. The driving force ΔG_{MeO} is, corresponding to the mole fraction N°_A or N°_B, smaller than for the oxidation of pure metals, and the mean value of the rate-determining diffusion coefficient in Equation (2) is likewise to be modified corresponding to the now applicable activities at the phase boundaries.

3.3 Development of Stable Surface Coatings

Along with the limiting case of alloy oxidation discussed in the previous section, for which $D_{Me} > D_i$(oxide), and the further limiting case in which transport in the alloy is essentially rate-determining for oxidation, so that the oxygen activity at the phase boundary is essentially that of the oxidizing gas, which leads to an unstable limiting surface and thus to a

phase conglomerate, we shall in this section determine when covering spinel coatings can occur with plane phase boundaries.

In his work [8] which has already been cited in another connection, Wagner has shown that steady activity values at the phase boundaries also occur in alloy oxidation if the single-phase oxide layer grows parabolically. This conclusion can be accepted directly for multi-phase coatings with plane phase boundaries. Now if we suppose that the system of differential equations for alloy oxidation has no solution under the initial and boundary conditions already formulated above, which leads to non-steady activity values and so to non-parabolic scales, then the following important question remains open: How does the oxidation process proceed up to the time where steady values of component activities have become regulated at the phase boundaries. Whether or not stable surface coatings can form from spinels depends on the course of this start-up process. From the viewpoint of the practitioner, Wood has made valuable studies. For the analysis of this problem in spinel formation, we consider an alloy (A, B) to which the phase diagram plotted in Figure 11 applies. Let the initial composition be N°_{B}, in which $N^{\circ}_{B} < N'_{B}$ and N''_{B}. If this alloy is caused to react in an oxidizing atmosphere at sufficiently high temperature, then we can read from Figure 11 that at first only AO forms as a surface coating ($D_{Me} > D_{i}$(oxide)!). Then at the metal/oxide boundary there is a depletion of A and an enrichment of B in comparison with the interior of the alloy. If the steady composition N^{st}_{B} which can be calculated formally from [8] is less than N°_{B}, then according to Figure 11, AB_2O_4 will form as soon as the alloy composition at the phase boundary reaches the value N'_{B}. Now Figure 12 portrays the moment at which the first nucleus of AB_2O_4 has formed, before it has grown to a complete surface coating. /380

Then the following distinctions must be applied: transport in the binary oxide AO is (1) rapid in comparison to the transport in the spinel and (2) slow in comparison to the transport in the spinel. For the reaction mechanism, it is yet to be established whether (a) $D^{Sp}_{A} \gg D^{Sp}_{B}$ in the spinel or (b) $D^{Sp}_{B} \gg D^{Sp}_{A}$ in the spinel.

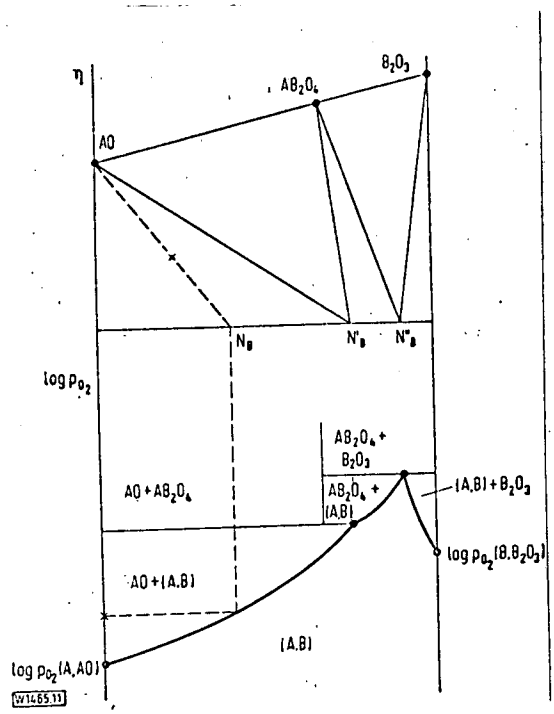

Figure 11. The phase diagram and the oxygen partial pressure in the ternary system A-B-O according to Figure 10,a.

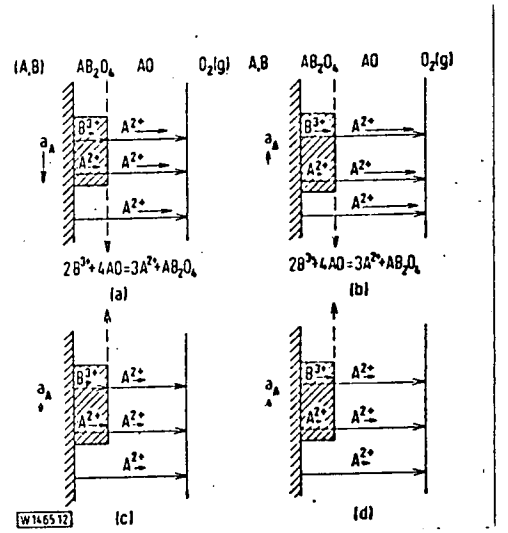

Figure 12. Reaction mechanisms after successful spinel nucleation in alloy oxidation. The flow of electron vacancies necessary for charge compensation is left out for clarity.

Let us begin with the case $D^{AO}_{A} \gg D^{Sp}_{A} \gg D^{Sp}_{B}$ (Figure 12,a). At the position of the metal/oxide boundary not yet covered with AB_2O_4, A will be broken down and transported to the phase boundary AO/gas, with final oxide formation. Thus the activity of B in the alloy will increase further and allow spinel formation. This increase in activity is also supported by the transport of A away through the spinel layer. This itself grows at the phase boundary AB_2O_4/AO by the transport of B slowly according to the reaction equation

$$2\,B^{3+} + 4\,AO = AB_2O_4 + 3\,A^{2+} \qquad (14)$$

in which the A^{2+} ions produced likewise diffuse to the AO/Gas phase boundary, there to react with oxygen. (Note that in this sense a reaction mechanism

proposed by Mrowee [26] for the formation of sulfo-spinels on Fe-Cr alloys can not be completely correct). In total, then, we record a relatively rapid growth of AO, a relatively slow growth of AB_2O_4 determined by D^{Sp}_B, and formation of a stable spinel layer. Even if the transport of A away from the alloy should finally lead to formation of B_2O_3 scale as a result of enrichment of B, the spinel layer remains stable. Under certain conditions it can even grow more through reaction between the outer AO and the inner B_2O_3. This further growth is not possible in every case, however. The condition for it is that the activity of AO at the phase boundary B_2O_3/AB_2O_4 according to Equation (4) must not sink below the value $\Delta G^\circ\ AB_2O_4/RT$.

If, in contrast to the case explained above, $D^{AO}_A \gg D^{Sp}_B \gg D^{Sp}_A$ (Figure 12,b), then a covering spinel layer is likewise formed at first, because where the spinel does not yet cover, an increase in the concentration of B in the alloy occurs due to the rapid transport of A away. But if a covering spinel layer has formed, then the spinel will grow primarily through diffusion of B^{3+} at the expense of AO according to the phase boundary reaction already formulated: $2\ B^{3+} + 4\ AO = AB_2O_4 + 3\ A^{2+}$ while the A^{2+} ions are rapidly carried away through the AO scale. But it is principally B which is removed from the alloy through this spinel growth, so that the alloy again becomes rich in A, and the spinel formation must finally stop. In this way, then, stable spinel growth is not possible. It will form alternately AO and AB_2O_4, i.e., a conglomerate of two oxide phases which initially becomes scale rapidly and remains limited by spinel formation. Mutual solubility of the oxides will modify this picture somewhat. In conjunction with the just-described growth mechanism, they are under some circumstances responsible for the concentration fluctuations in scale spinel layers found experimentally [27].

Both the latter limiting cases (Figure 12,c and d) introduce nothing basically new. If $D^{Sp}_A \gg D^{AO}_A \gg D^{Sp}_B$, then, as can easily be seen, there again results a stable covering spinel layer, because at anytime more A than B is removed from the alloy. On the other hand, if $D^{Sp}_B \gg D^{AO}_A \gg D^{Sp}_A$, then after

initial AO scaling and the AB_2O_4 formation which follows it, the spinel will grow at the expense of AO. In this way the alloy will again become rich in A at the phase boundary with the oxide, thus interrupting the spinel formation according to Figure 11.

In agreement with this discussion, no problems arise in the complementary case of alloy oxidation when $|\Delta G^\circ_{B_2O_3}| \gg |3\,\Delta G^\circ_{AO}|$ so that Figure 10,b applies instead of Figure 10,a or 11, and B_2O_3 appears as the covering layer instead of AO at the beginning of oxidation.

3.4 Some Comments on Observations Reported in the Literature.

From the beginning, it has appeared very practical for the discussion of experimental results in alloy oxidation systems to differentiate between the stage of regulated steady thermodynamic equilibrium at all phase boundaries and the processes which occur before that. Wood [25] properly states that the morphologic structures which form in the initial transition stages also affect the steady-state activity values of the components at the phase boundaries and thus the entire kinetics.

Since these morphologic structures can separate quite differently, depending on the oxidation temperature, activity of the oxidizing gas, alloy, alloy composition, geometry and pretreatment of the sample, it is quite difficult to make generally applicable determinations with respect to spinel formation in scale layers. In any case, it is expedient, for evaluation of the thermodynamic realities, to sketch phase diagrams of the type of Figure 11 (η/N_B and $\log pO_2/N_B$ with $\eta = n_O/n_A + n_B$). They indicate which oxide will form first in the scale, what partial pressure of oxygen prevails at the alloy/scale phase boundary, and also — if the steady-state values of alloy composition are theoretically accessible [8] — which phase sequences are to be expected in the initial transition stage.

Steady values of the component activities in the proper sense can occur only at plane stable phase boundaries. Under such circumstances parabolic growth

kinetics are to be expected. But somewhat parabolic growth of the scale layer thickness frequently occurs even with non-plane phase boundaries.

The occurrence of uneven spinel layers in scales and, linked with that, the appearance of conglomerates of different oxides adjacent in the scale layer have essentially two causes. (1) The stable binary or ternary oxide forms through internal oxidation. Correspondingly, the alloy becomes depleted in the metallic portion. The second oxide formed by external oxidation grows over the oxide particles of the inner oxidation. Under some circumstances, it reacts with this to become spinel. Depending on the solubility of the oxides with respect to each other, and depending on the relative quantity fraction and processes in the advancing phase boundary, it is possible for almost hermetic spinel covering layers to be produced. Depending on the transport properties in comparison with the binary oxide of the external oxidation, they can have a lesser or greater corrosion retarding effect. A good example of this was given by Kofstad [32] for the system Co-Cr-O in an experiment. Similar observations are available for Ni-Cr-O and Fe-Cr-O [33, 34]. Based on the diffusion coefficients shown in Figure 7, for the system Co-Cr-O it is to be expected that the $CoCr_2O_4$ which is formed will reduce the oxidation rate by reducing the diffusion cross section of CoO. However, one must be careful with transferring the cation final diffusion coefficient of the spinel measured in air. As was shown in Section 2.4, the transport coefficient of spinels from transition metal oxides can have a strong dependence on the oxygen pressure. The oxygen activity at the phase boundary alloy/CoO is relatively low and can be read off state diagrams of the type shown in Figure 11. A further remark should be made in this connection. The solubility of Cr_2O_3 in FeO, NiO and CoO was determined [34] using the microsond. These solubilities refer to the binary oxides for relatively low, but unknown, oxygen partial pressures and cannot be directly compared with the solubilities for other oxygen pressures [35].

(2) Nonplanar spinel layers and subsequent phase conglomerates also occur if the transport is primarily being determined in the alloy by means of the reaction rate. The conditions for this have been given by Wagner [6]. In practice it is to be expected that a certain unevenness at the phase boundary alloy/scale will have a positive effect on the adhesion capacity of the scale, especially if they occur in the submicroscopic range.

In addition to the described spinel layers which have an uneven structure, there is continuously reference to planar covering spinels in the literature. These can have a corrosion protection effect if their diffusion coefficients shown in Figure 7 were to lie considerably lower than those of the other oxides in the scale layer. If such a spinel occurs in addition to Al_2O_3 [36], Cr_2O_3 [34] or even Fe_2O_3, then its protective effect can be only small or possibly comparable with these oxides, if there are no other factors such as improvement of the adhesion capacity, etc. It should be noted that the formation of covering spinel layers which grow in a stationary manner assumes that $3\,\Delta\,G°AO$ and $\Delta\,G°_{B_2O_3}$ are not too different from each other, in addition to the condition that the scale rate depends essentially on the oxide layer. Otherwise, the values N'_B and N''_B, which according to Equation (11) encompass the range of existence of the alloy in equilibrium with the spinel phase, become extremely small or large, i.e., they either go to zero or to 1.

With the above discussion, it is now easy to formulate the condition which is the prerequisite for the occurrence of a single spinel phase alone during the entire scale process: this condition is $3\,|\Delta G°_{AO}| \cong |\Delta G°_{B_2O_3}|$, where the state diagram shown in Figure 11 would have to be modified, as shown in Figure 13.

In this connection, we should mention a paper by Douglass [37], which describes the oxidation of Ni-20-Cr alloys, in the case where 1 - 3% of manganese is added. The external phase sequences NiO, $NiCr_2O_4$, CR_2O_3 are not clear. However, the covering $MnCr_2O$ layer can be detected on the alloy. Since, (in contrast to [37]) MnO has a somewhat lower standard value of the

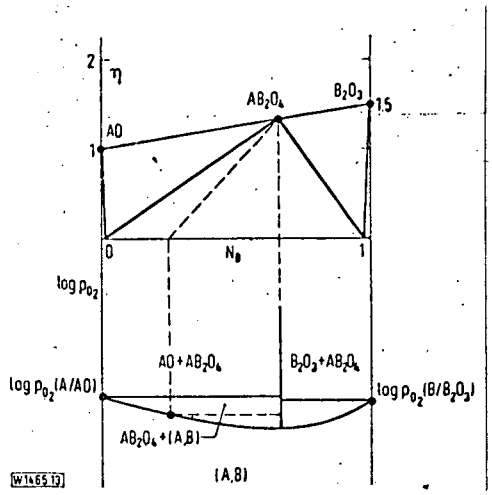

Figure 13. The state diagram and the oxygen partial pressures in the ternary system A-B-O (see also Figure 10), for the case $3\,\Delta G^\circ_{AO} \simeq \Delta G^\circ_{B_2O_3}$

free formation enthalpy than 1/3 $Cr_2{}_3$, the thermal dynamic formation of $MnCr_2O_4$ in spite of the relatively low manganese content of the alloy immediately becomes understandable according to what was said above. We should not expect that $MnCr_2O_4$ offers a better oxidation protection compared with Cr_2O_4. The published kinetic data do not make it possible to make a decisive statement in this regard. However, if in similar cases a reduction of the scale velocity is detected, then there is the possibility that because of the change of the oxygen partial pressure at the phase boundary AB_2O_4/B_2O_3 with respect to $(A, b)/B_2O_3$, the ion transport in B_2O_3 can be very strongly influenced. A last word of caution: reaction constants of spinel formation have been determined for constant oxygen potentials. Therefore it is not permissible to directly compare them with the spinel formation in scale layers in most cases, because not only does the activity of the binary oxides in spinel vary locally, but at the same time, the oxygen activity and also these values at the phase boundaries can only be determined in the rarest cases.

Finally, we would like to emphasize again that the conclusions regarding oxide-spinel formation in scale layers can be immediately applied to other ternary ion compounds (such as sulfospinels [26] or silicates) in the corresponding form.

REFERENCES

1. *P. Kofstad:* High Temperature Oxidation of Metals, Wiley, New York 1967.
2. *G. Tammann:* Z. anorg. allg. Chemie *111*, 78 (1920).
3. *N. B. Pilling* und *R. E. Bedworth:* J. Inst. Metals *29*, 529 (1923).
4. *C. Wagner:* Z. phys. Chemie *B 21*, 25 (1933).
5. *H. Schmalzried:* Festkörperreaktionen, Verlag Chemie, Weinheim 1971.
6. *C. Wagner:* Ber. Bunsenges. phys. Chemie *63*, 772 (1959).
7. *C. Wagner:* Corrosion Science *9*, 91 (1969).
8. *C. Wagner:* J. Electrochem. Soc. *99*, 369 (1952).
9. *C. Wagner:* J. Electrochem. Soc. *103*, 571 (1956).
10. *E. W. Gorter:* Philips Res. Repts. *9*, 295 (1954).
11. *F. C. M. Driessens:* Ber. Bunsenges. phys. Chemie *72*, 764 (1968).
12. *G. Blasse:* Philips Res. Repts. Suppl. No. 3, 1964.
13. *P. V. Ribond* und *A. Muan:* Trans. AIME *230*, 88 (1964).
14. *D. M. Roy, R. Roy* und *E. F. Osborn:* J. Am. Cer. Soc. *36*, 149 (1953).
15. *H.-G. Sockel* und *H. Schmalzried:* Ber. Bunsenges. phys. Chemie *72*, 745 (1968).
16. *J. D. Tretjakov* und *H. Schmalzried:* Ber. Bunsenges. phys. Chemie *69*, 396 (1965).
17. *F. A. Kröger:* Chemistry of Imperfect Crystals, North-Holland Publ. Comp., Amsterdam 1964.
18. *H. Schmalzried,* Point Defects in Ternary Ionic Crystals, in „Progress in Solid State Chemistry", H. Reiss, Herausgeber, Vol. 2, Pergamon Press, New York 1965.
19. *W. Müller* und *H. Schmalzried:* Ber. Bunsenges. phys. Chemie *68*, 270 (1964).
20. *B. D. Lichter* und *C. W[illegible]*, J. Electrochem. Soc. *107*, 168 (1960).
21. *H. Schmalzried:* Reactivity of Solids, J. W. Mitchell et al., Editors, Wiley, New York 1969.
22. *G. C. Wood:* Oxidation of Metals *2*, 11 (1970).
23. *H. H. Hohmann et al.:* Proc. Brit. Cer. Soc. *8*, 91 (1967).
24. *Y. Adda* und *J. Philibert:* La Diffusion dans les Solides, Vol. II, Presses Universitaires de France, S. 1128 ff.
25. *B. Chattopadhyay* und *G. C. Wood:* Oxidation of Metals *2*, 373 (1970).
26. *S. Mrowec et al.:* Bulletin de l'Académie Polonaise des Sciences, Ser. Chim. *5*, 261 (1968).
27. *D. P. Whittle* und *G. C. Wood:* J. Electrochem. Soc. *114*, 992 (1967).
28. *H. Rickert* und *C. Wagner:* Z. Elektrochem. *64*, 793 (1960).
29. *G. Zintl:* Z. phys. Chemie NF *48*, 340 (1966).
30. *H. Schmalzried* und *J. B. Holt:* Z. phys. Chemie NF *60*, 220 (1968).
31. *C. Greskovich* und *H. Schmalzried:* J. Phys. Chem. Solids *31*, 639 (1970).
32. *P. Kofstad* und *J. Hed:* J. Electrochem. Soc. *116*, 1542 (1969).
33. *D. L. Douglass:* Corrosion Science *8*, 665 (1968).
34. *G. C. Wood et al.:* A Comparison of the Oxidation of Fe-Cr, Ni-Cr and Co-Cr-Alloys in Oxygen and Water Vapour, to be published.
35. *C. Greskovich:* J. Am. Cer. Soc. *53*, 498 (1970).
36. *F. S. Pettit:* Trans. AIME *239*, 1296 (1967).
37. *D. L. Douglass* und *J. S. Armijo:* Oxidation of Metals *2*, 207 (1970).

Translated for National Aeronautics and Space Administration under Contract No. NASw 2035, by SCITRAN, P.O. BOX 5456, Santa Barbara, California, 93108